# Numerical Simulation of Vortex-Dipole Wall Interactions Using an Adaptive Wavelet Discretization with Volume Penalisation

Kai Schneider[1] and Marie Farge[2]

[1] LMSNM–CNRS & CMI, Université de Provence, 39 rue Joliot–Curie, 13453 Marseille cedex 13, France
kschneid@cmi.univ-mrs.fr
[2] LMD–CNRS, Ecole Normale Supérieure, 24 rue Lhomond, 75231 Paris cedex 05, France
farge@lmd.ens.fr

**Summary.** We present an adaptive wavelet method for solving the incompressible Navier–Stokes equations in two space dimensions using the vorticity-stream function formulation. For time discretization a semi–implicit scheme of second order is used. The space discretization is based on a Petrov–Galerkin method, where orthogonal spline wavelets of 4th order are employed as trial functions and operator adapted wavelets as test functions. The no–slip boundary conditions are imposed using a volume penalisation method. As example we present adaptive simulations of vortex-dipole wall interactions.

## 1 Introduction

The mathematical properties of wavelets (see, *e.g.,Daub92*) motivate their use for the numerical solution of partial differential equations (PDEs). The localization of wavelets, both in scale and space, leads to effective sparse representations of functions and pseudo–differential operators (and their inverse) by performing nonlinear thresholding of the wavelet coefficients of the function and of the matrices representing the operators. Estimating the local regularity of the solution of the PDE auto–adaptive discretizations with local mesh refinements can be defined. The characterization of function spaces in terms of wavelet coefficients and the corresponding norm equivalences allow diagonal preconditioning of operators in wavelet space. Finally, the existence of the fast wavelet transform yields algorithms with optimal linear complexity.

The currently existing algorithms can be classified in different ways. We can distinguish between Galerkin, collocation schemes and algebraic wavelet methods. By the latter we mean algorithms which start from a classical discretization, e.g. by finite differences or finite volumes. Wavelets are then used

to speed up the linear algebra and to define adaptive grids. On the other hand the former two schemes employ wavelets directly for the discretization of the solution and the operators. For an overview on wavelet methods we refer the reader to [5, 4].

Wavelet methods have been developed to solve Burger's equation, Stokes' equation, Kuramoto–Sivashinsky equation, the nonlinear Schrödinger equation, the Euler and Navier–Stokes equations.

In the follwing we present an adaptive wavelet algorithm of Galerkin type [10] to solve the two–dimensional Navier–Stokes equation in vorticity–stream function formulation. The boundary conditions are imposed using a volume penalisation technique. As application we present computations of a vortex dipole impinging on a no-slip wall in a square container at Reynolds number 1000, which is a challenging test case for numerical methods [12, 3]. Finally, we present some conclusions and perspectives for future work.

## 2 Adaptive wavelet discretization with volume penalisation

### 2.1 An adaptive wavelet scheme

The volume penalisation method has been proposed by Arquis and Caltagirone [1]. Its is based on the physical idea which consists in modelling solid walls or obstacles as porous media whose porosity $\eta$ tends to zero. The geometry of the flow is described by a mask function $\chi$. The incompressible Navier-Stokes equations are modified by adding a forcing term containing the mask function. Using vorticity $\omega$ and the stream function $\Psi$, which are both scalars in 2d, the equations are:

$$\partial_t \omega + \mathbf{v} \cdot \nabla \omega - \nu \nabla^2 \omega = \nabla \times \mathbf{F} \tag{1}$$

$$\nabla^2 \Psi = \omega \quad \text{and} \quad \mathbf{v} = \nabla^\perp \Psi \tag{2}$$

for $\mathbf{x} \in \Omega$ , $t > 0$. The velocity is denoted by $\mathbf{v}$, $\nu > 0$ is the constant kinematic viscosity and $\nabla^\perp = (-\partial_y, \partial_x)$. The fluid region $\Omega_f$ is embedded in the enlarged domain $\Omega$ containing in addition a solid region $\Omega_s$ which is surrounding the fluid region. The penalisation term $\mathbf{F} = -\frac{1}{\eta} \chi_{\Omega_s} \mathbf{v}$ imposes no–slip boundary conditions on the walls, corresponding to the interface between the fluid and solid region, i.e. $\Omega_f$ and $\Omega_s$, respectively. The mask function $\chi$ is defined as

$$\chi_{\Omega_s}(\mathbf{x}) = \begin{cases} 1 & \text{for} \quad \mathbf{x} \in \bar{\Omega}_s, \\ 0 & \text{elsewhere} \end{cases} \tag{3}$$

where $\Omega_s$ denotes the ensemble of solid obstacles. The above equations are completed with a suitable initial condition.

In [2] it has been shown rigorously that the penalised equations written in primitive variables converge towards the Navier–Stokes equations with no-slip boundary conditions, with order $\eta^{3/4}$ inside the obstacle and with order $\eta^{1/4}$ elsewhere, in the limit when $\eta$ tends to zero. In numerical simulations an improved convergence of order $\eta$ has been reported [2, 11].

### Time discretization

Introducing a classical semi–implicit time discretization with a time step $\delta t$ and setting $\omega^n(\mathbf{x}) \approx \omega(\mathbf{x}, n\delta t)$ we obtain

$$(1 - \nu\delta t\nabla^2)\omega^{n+1} = \omega^n + \delta t(\nabla \times F^n - \mathbf{v}^n \cdot \nabla\omega^n) \tag{4}$$

$$\nabla^2\Psi^{n+1} = \omega^{n+1} \quad \text{and} \quad \mathbf{v}^{n+1} = \nabla^\perp\Psi^{n+1} \tag{5}$$

Hence in each time step two elliptic problems have to be solved and a differential operator has to be applied. Formally the above equations can be written in the abstract from $Lu = f$, where $L$ is an elliptic operator with constant coefficients, corresponding to a Helmholtz type equation for $\omega$ with $L = (1 - \nu\delta t\nabla^2)$ and a Poisson equation for $\Psi$ with $L = \nabla^2$.

In practice we use a time scheme composed of an Euler–Backwards scheme and an Adams–Bashforth scheme, both of second order [10].

### Spatial discretization

For the spatial discretization we use the method of weighted residuals, *i.e.*, a Petrov–Galerkin scheme. The trial functions are orthogonal wavelets and the test functions are operator adapted wavelets. To solve the elliptic equations $Lu = f$ at time step $t^{n+1}$ we develop $u^{n+1}$ into an orthogonal wavelet series, *i.e.*, $u^{n+1} = \sum_\lambda \widetilde{u}_\lambda^{n+1}\psi_\lambda$, where $\lambda = (j, i_x, i_y, d)$ denotes the multi–index containing scale, space and direction information. Requiring that the residuum vanishes with respect to all test functions $\theta_{\lambda'}$, we obtain a linear system for the unknown wavelet coefficients $\widetilde{u}_\lambda^{n+1}$ of the solution $u$:

$$\sum_\lambda \widetilde{u}_\lambda^{n+1} \langle L\psi_\lambda \, , \, \theta_{\lambda'} \rangle = \langle f \, , \, \theta_{\lambda'} \rangle. \tag{6}$$

The test functions $\theta$ are defined such that the stiffness matrix turns out to be the identity. Therefore the solution of $Lu = f$ reduces to a change of the basis, *i.e.*, $u^{n+1} = \sum_\lambda \langle f \, , \, \theta_\lambda \rangle \psi_\lambda$.

The right-hand side $f$ can then be developed into a biorthogonal operator adapted wavelet basis $f = \sum_\lambda \langle f \, , \, \theta_\lambda \rangle \mu_\lambda$, with $\theta_\lambda = L^{\star-1}\psi_\lambda$ and $\mu_\lambda = L\psi_\lambda$ ($^\star$ denotes the adjoint operator). By construction $\theta$ and $\mu$ are biorthogonal, $\langle \theta_\lambda \, , \, \mu_{\lambda'} \rangle = \delta_{\lambda,\lambda'}$. It can be shown that both have similar localization properties in physical and Fourier space as has $\psi$ and that they form a Riesz basis [10].

*Adaptive discretization*

To get an adaptive space discretization for the problem $Lu = f$ we consider only the significant wavelet coefficients of the solution. Hence we only retain coefficients $\widetilde{u}_\lambda^n$ which have an absolute value larger than a given threshold $\varepsilon$, *i.e.*, $|\widetilde{u}_\lambda^n| > \varepsilon$. The corresponding coefficients are shown in Fig.1 (white area under the solid line curve).

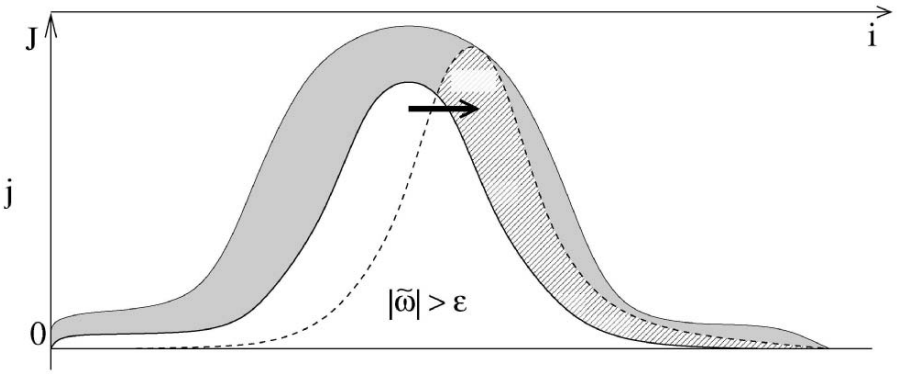


**Fig. 1.** Illustration of the dynamic adaption strategy in wavelet coefficient space.

*Adaption strategy*

To be able to integrate the equation in time we have to account for the evolution of the solution in wavelet coefficient space (indicated by the arrow in Fig. 1). Therefore we add at time step $t^n$ the local neighbors to the retained coefficients, which constitute a security zone (grey domain in Fig.1). The equation is then solved in this enlarged coefficient set (white and grey region in Fig.1) to obtain $\widetilde{u}_\lambda^{n+1}$. Subsequently we threshold the coefficients and retain only those with $|\widetilde{u}_\lambda^{n+1}| > \varepsilon$ (coefficients under the dashed curve in Fig.1 ). This strategy is applied in each time step and allows hence to track automatically the evolution of the solution in scale and space.

*Evaluation of the nonlinear term*

For the evaluation of the nonlinear term $f(u^n)$, where the wavelet coefficients of $u^n$ are given, there are two possibilities:

- evaluation in wavelet coefficient space.
  As illustration we consider a quadratic nonlinear term, *i.e.*, $f(u) = u^2$. The wavelet coefficients of $f$ can be calculated using the connection coefficients, *i.e.*, one has to calculate the bilinear expression, $\sum_\lambda \sum_{\lambda'} \widetilde{u}_\lambda T_{\lambda\lambda'\lambda''} \widetilde{u}_{\lambda'}$

with the interaction tensor $T_{\lambda\lambda'\lambda''} = \langle \psi_\lambda \, \psi_{\lambda'}, \theta_{\lambda''} \rangle$. Although many coefficients of $T$ are zero or very small, the size of $T$ leads to a computation which is quite untractable in practice.

- evaluation in physical space.
  This approach is similar to the pseudo-spectral evaluation of nonlinear terms used in spectral methods, and therefore this method is called pseudo–wavelet technique. The advantage of this scheme is that more general nonlinear terms, *e.g.*, $f(u) = (1-u)\, e^{-C/u}$, can be treated more easily. The method can be summarized as follows: starting from the significant wavelet coefficients of $u$, *i.e.*, $|\widetilde{u}_\lambda| > \varepsilon$, one reconstructs $u$ on a locally refined grid, $u(x_\lambda)$. Then one can evaluate $f(u(x_\lambda))$ pointwise and the wavelet coefficients of $f$ can be calculated using the adaptive decomposition to get $\widetilde{f}_\lambda$.

Finally, we have to calculate those scalar products of the r.h.s $f$ with the test functions $\theta$, to advance the solution in time. We compute $\widetilde{u}_\lambda = \langle f, \theta_\lambda \rangle$ belonging to the enlarged coefficient set (white and grey region in Fig. 1).

In summary the above algorithm is of $O(N)$ complexity, where $N$ denotes the number of wavelet coefficients used in the computation.

## 3 Vortex-dipole wall interactions

To illustrate the above algorithm we present an adaptive wavelet computation of a vortex–dipole impinging on a no-slip wall at Reynolds number $Re = 1000$ in a square container with $Re = \frac{\overline{u}L}{\nu}$ and where $\overline{u}$ denotes the rms velocity of the flow, $L$ the half-width of the container and $\nu$ the kinematic viscosity. The Navier-Stokes equations are solved in a periodic square domain of size 2.2 in which the square container $[-1, 1]^2$ is imbedded. The no slip boundary conditions are imposed using a volume penalisation method. The porosity $\eta$ is $10^{-3}$ and the maximal numerical resolution is $1024^2$. The initial vorticity distribution of the two isolated monopoles is given by

$$\omega(r, t=0) = \omega_0 \left(1 - \left(\frac{r}{r_0}\right)^2\right) \exp\left(-\left(\frac{r}{r_0}\right)^2\right) \tag{7}$$

where $r$ is the distance from the center of the monopole. Following [3] we chose $r_0 = 0.1$ and $\omega_0 = \pm 320$. The initial position of the two isolated monopoles is $\{(x_1, y_1), (x_2, y_2)\} = \{(0, 0.1), (0, -0.1)\}$.

Figure 2 (left) shows snapshots of the vorticity field at times $t = 0.2, 0.4, 0.6$ and 0.8. We observe that the dipole is moving towards the wall and that strong vorticity gradients are created when it hits the wall. The computational grid is dynamically adapted during the flow evolution, since the nonlinear wavelet filter automatically refines the grid in regions where strong gradients develop.

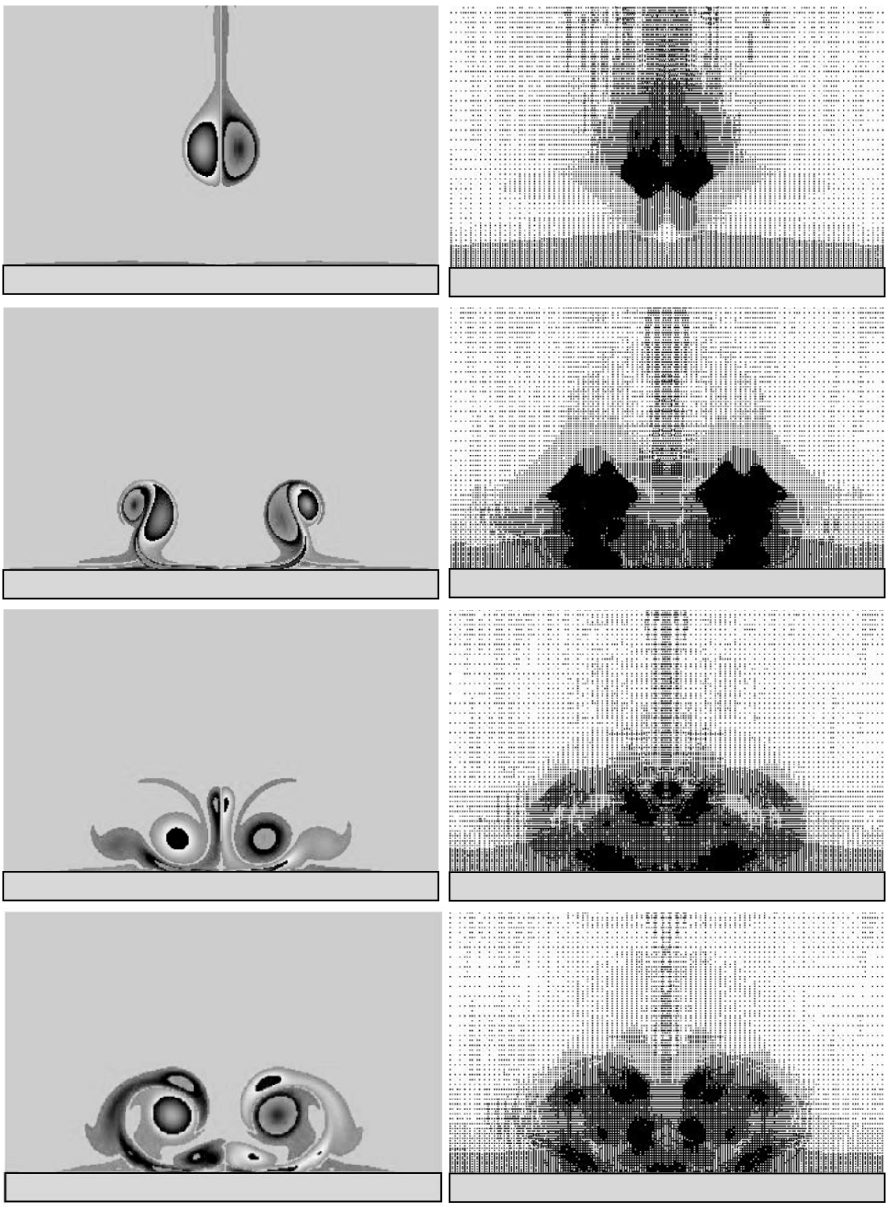

**Fig. 2.** Dipole–wall interaction at $Re = 1000$. Vorticity fields (left), corresponding centers of active wavelets (right), at $t = 0.2, 0.4, 0.6$ and $0.8$ (from top to bottom).

Figure 2 (right) shows the centers of the retained wavelet coefficients at corresponding times. Note that during the computation only 5% out of $1024^2$ wavelet coefficients are thus used. The time evolutions of total kinetic energy

$E(t) = \frac{1}{2}\int_{-1}^{1}\int_{-1}^{1} \mathbf{v}^2 dxdy$ and total enstrophy $Z(t) = \frac{1}{2}\int_{-1}^{1}\int_{-1}^{1} \omega^2 dxdy$ are plotted in Fig. 3 to illustrate the production of enstrophy and the dissipation of energy when the dipole is hitting the wall.

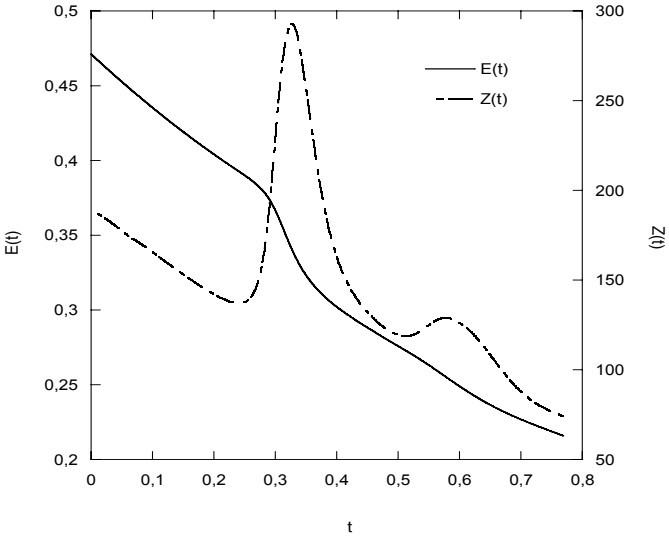


**Fig. 3.** Time evolution of energy (solid line) and enstrophy (dotted line).

## 4 Conclusions

In conclusion, we have checked the ability of the adaptive wavelet solver to track the evolution of the dipole and its nonlinear interaction with the no-slip wall. The utilisation of a volume penalisation method enables us to take into account complex geometries using a mask function, without modifying the numerical scheme and the underlying grid. The precision of the method is determined by the penalisation parameter $\eta$ which can be chosen a priori. An explicit time discretization of the penalisation term implies, however, a time step smaller than $\eta$ to guarantee stability of the numerical scheme. We have shown that this approach is suitable to model walls even in the case of strong interaction with vortices.

The adaptive wavelet method presented in this paper allows automatic grid generation and refinement near the wall and also in shear layers which develop during the flow evolution. Therewith, the number of required grid–points in the simulations is significantly reduced. We conjecture that the compression rate thus obtained increases with the Reynolds number. Current work is

dealing with the development of adaptive local time stepping using a Runge–Kutta–Fehlberg method in order to control the error of the scheme in time [7].

In future work we will extend the penalisation scheme to compute three–dimensional flows and perform computations at high Reynolds numbers using the Coherent Vortex Simulation approach (CVS), proposed in [8, 9]. Applications to 3d turbulent mixing layers have been presented in [14].

## Acknowledgements

We thankfully acknowledge financial support from the European Union project IHP on 'Breaking complexity'.

## References

1. Arquis, E. Caltagirone, J.-P.: Sur les conditions hydrodynamiques au voisinage d'une interface milieu fluide – milieux poreux: application à la convection naturelle.
   Comptes Rendus de l'Academie des Sciences, Paris, II **299**, 1–4 (1984)
2. Angot, P., Bruneau, C.-H., Fabrie, P.: A penalisation method to take into account obstacles in viscous flows. Num. Math., **81**, 497–520 (1999)
3. Clercx, H.J.H., van Heijst G.J.F.: On the dissipation of energy in 2D turbulence in a bounded domain, Adv. in Turbulence IX, CIMNE, Barcelona, 773–776 (2002)
4. Cohen, A.: Wavelet methods in numerical analysis. Handbook of Numerical Analysis. Eds. P.G. Ciarlet & J.L. Lions, Vol. 7, Elsevier, Amsterdam (2000)
5. Dahmen, W.: Wavelets and multiscale methods for operator equations. Acta Numerica, **6**, 55–228, Cambridge University Press (1997)
6. Daubechies, I.: Ten lectures on wavelets. SIAM (1992)
7. Domingues, M.O., Roussel, O., Schneider, K.: A time and space adaptive multiresolution scheme for parabolic PDEs. Preprint CMI, Marseille (2005), submitted.
8. Farge, M., Schneider, K., Kevlahan N.: Non–Gaussianity and Coherent Vortex Simulation for two–dimensional turbulence using an adaptive orthonormal wavelet basis, Phys. Fluids, **11**(8), 2187–2201 (1999)
9. Farge, M., Schneider, K.: Coherent Vortex Simulation (CVS), a semi–deterministic turbulence model using wavelets. Flow, Turbulence and Combustion **66**(4), 393–426 (2001)
10. Fröhlich, J., Schneider, K.: An adaptive wavelet–vaguelette algorithm for the solution of PDEs. J. Comput. Phys., **130**, 174–190 (1997)
11. Kevlahan, N., Ghidaglia, J.-M.: Computation of turbulent flow past an array of cylinders using a spectral method with Brinkman penalization. Eur. J. Mech./B, **20**, 333–350 (2001)
12. Orlandi, P.: Vortex dipole rebound from a wall. Phys. Fluids A **2**(8), 1429–1436 (1990)

13. Schneider, K., Farge, M.: Adaptive wavelet simulation of a flow around an impulsively started cylinder using penalisation. Appl. Comput. Harm. Anal., **12**, 374–380 (2002)
14. Schneider, K., Farge, M., Pellegrino, G., Rogers, M.: Coherent vortex simulation of three–dimensional turbulent mixing layers using orthogonal wavelets. J. Fluid Mech., **534**, 39–66 (2005)
15. Schneider, K.: Numerical simulation of the transient flow behaviour in chemical reactors using a penalisation method. Computers and Fluids, **34**, 1223–1238 (2005)